Mathematical Biosciences and Engineering

MBE, 18(6): 7619–7630.
DOI: 10.3934/mbe.2021377
Received: 07 August 2021
Accepted: 25 August 2021
Published: 03 September 2021

http://www.aimspress.com/journal/MBE

Research article

Identification of ferroptosis-associated genes exhibiting altered expression in pulmonary arterial hypertension

Fan Zhang[1] and Hongtao Liu[2,*]

[1] Department of Anesthesiology, Renmin Hospital of Wuhan University, Wuhan 430060, China.
[2] Department of Anesthesiology, The First Affiliated Hospital, Jinan University, Guangzhou 510632, China

* **Correspondence:** Email: lhtgood@sina.com; Tel: +8615977470206.

Abstract: Pulmonary arterial hypertension (PAH) is a life-threatening illness and ferroptosis is an iron-dependent form of regulated cell death, driven by the accumulation of lipid peroxides to levels that are sufficient to trigger cell death. However, only few studies have examined PAH-associated ferroptosis. In the present study, lung samples mRNA expression profiles (derived from 15 patients with PAH and 11 normal controls) were downloaded from a public database, and 514 differentially expressed genes (DEGs) were identified using the Wilcoxon rank-sum test and weighted gene correlation network analyses. These DEGs were screened for ferroptosis-associated genes using the FerrDb database: eight ferroptosis-associated genes were identified. Finally, the construction of gene-microRNA (miRNA) and gene-transcription factor (TF) networks, in conjunction with gene ontology and biological pathway enrichment analysis, were used to inform hypotheses regarding the molecular mechanisms underlying PAH-associated ferroptosis. Ferroptosis-associated genes were largely involved in oxidative stress responses and could be regulated by several identified miRNAs and TFs. This suggests the existence of modulatable pathways that are potentially involved in PAH-associated ferroptosis. Our findings provide novel directions for targeted therapy of PAH in regard to ferroptosis. These findings may ultimately help improve the therapeutic outcomes of PAH.

Keywords: Pulmonary arterial hypertension; ferroptosis; FerrDb; miRNA; TFs

1. Introduction

Pulmonary arterial hypertension (PAH) is a life-threatening illness, which leads to a progressive

increase in pulmonary vascular resistance and right heart failure. There are several subgroups of PAH including: idiopathic PAH, hereditary PAH, drug or toxins-induced PAH, PAH associated with congenital heart diseases, infective disease, etc. [1]. It seems, therefore, the underlying mechanisms and clinical classification of PAH are complex and the pathogenic factors are diverse. Although BMPR2 (bone morphogenetic protein type 2 receptor) and SOX17 (SRY-related high-mobility group box family member 17) are associated with PAH [2,3], the etiopathogenesis remain largely unclear.

Ferroptosis is an iron-dependent form of regulated cell death, driven by the accumulation of lipid peroxides to levels that are sufficient to trigger cell death [4]. It is linked to several lung diseases, such as acute lung injury and lung fibrosis [5,6]. However, only few studies have examined ferroptosis in the context of PAH.

In the present study, lung samples mRNA expression profiles [7] (15 with PAH: 6 idiopathic PAH, 4 connective tissue disease and 4 congenital heart disease and in 1 chronic thromboembolic PH, and 11 normal lung samples) were downloaded from a publicly accessible database. Next, differentially expressed genes (DEGs) were identified and screened for ferroptosis-associated genes. Finally, functional enrichment analysis and construction of gene-microRNA (miRNA) and gene-transcription factor (TF) networks facilitated exploration of molecular mechanisms underlying PAH-associated ferroptosis. If validated further, our findings will provide a new direction for the treatment of PAH, and contribute to improving the therapeutic outcomes following PAH.

2. Materials and methods

2.1. Data acquisition

The gene expression dataset GSE113439 (platform: GPL6244) was downloaded from the Gene Expression Omnibus database (https://www.ncbi.nlm.nih.gov/geo/) [8]. This dataset included lung samples mRNA expression profiles derived from 15 patients with PAH (fresh frozen lung samples obtained from the recipients organs) and 11 normal controls (normal lung tissue obtained from tissue flanking lung cancer resections). The R project for statistical computing (v3.6) [9] was used in conjunction with the R package limma [10] to normalize the raw data.

2.2. Identification of DEGs

*The base R function wilcox.test was used to apply the Wilcoxon rank-sum test to identify DEGs. The R packages ggplo*t2 [11] and pheatmap [12] were used to generate a volcano plot and heatmap, respectively. Statistical significance thresholds for differential expression were set at $p < 0.05$ and $|\log2 \text{ fold-change}| > 1$.

2.3. Weighted gene correlation network analysis (WGCNA)

A weighted correlation network analysis was performed using expression data to find clusters (modules) of highly correlated genes [13]. The best soft threshold power value was automatically selected by the software, then the co-expression networks were constructed and disease-associated modules were identified using the R package WGCNA [13]. In order to identify key DEGs, the R package VennDiagram [14] was used to construct Venn diagrams demonstrating the intersection of

DEGs and key modules.

2.4. Screening for ferroptosis-associated genes

A list of ferroptosis-associated genes was downloaded from FerrDb, the world's first database of ferroptosis regulators and markers, as well as ferroptosis-disease associations [15]. The list contained gene drivers (promote ferroptosis), suppressors (prevent ferroptosis), and markers (altered expression indicates the occurrence of ferroptosis). The R package VennDiagram [14] was used to construct Venn diagrams demonstrating the intersection of key DEGs and all ferroptosis-associated genes, as well as (separately) the intersection of key DEGs and drivers, suppressors, and markers. In this manner, pre- and post-CPB ferroptosis-associated genes were identified. The R packages beeswarm [16] and ggpubr [17] were used to draw boxplots demonstrating differential expression levels of ferroptosis-associated genes in the pre- and post-CPB groups. Finally, a correlation heatmap of ferroptosis-associated genes was generated using Pearson correlation analysis as provided by Sangerbox tools, a free online platform for data analysis (http://www.sangerbox.com/tool).

2.5. Functional enrichment analysis

The R package clusterProfile [18] was used to conduct gene ontology (GO) term [19] and Kyoto Encyclopedia of Genes and Genomes (KEGG) biological pathway [20] enrichment analyses of PAH-altered ferroptosis-associated genes. In addition, a pathway diagram of ferroptosis-associated genes was downloaded from FerrDb.

2.6. Construction and analysis of gene-miRNA and gene-TF networks

NetworkAnalyst (https://www.networkanalyst.ca/) was used to integrate miRTarBase (miRNA) [21] and ENCODE (TF) [22] databases. Nodes with degree ≥ 3 were extracted to construct and visualize ferroptosis-associated gene-miRNA and gene-TF networks using the Cytoscape [23] plugin. An overview of the complete study workflow is provided in Figure 1.

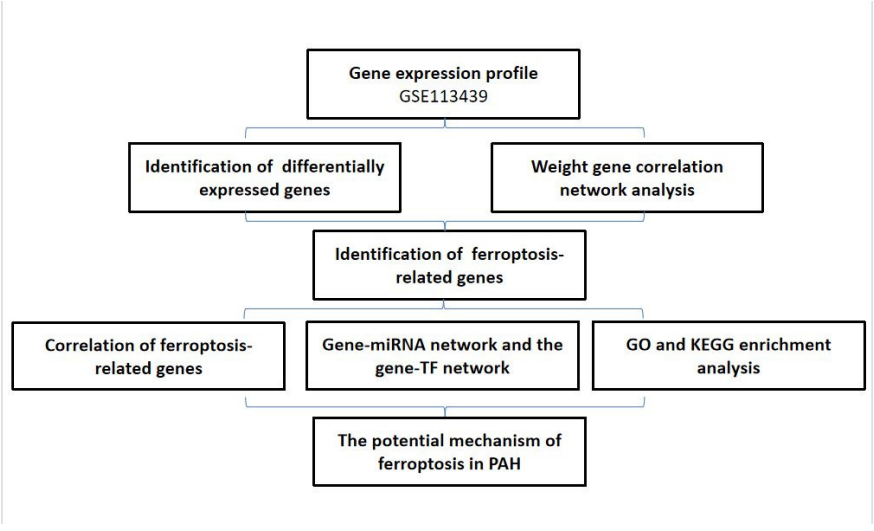

Figure 1. The workflow of the present study.

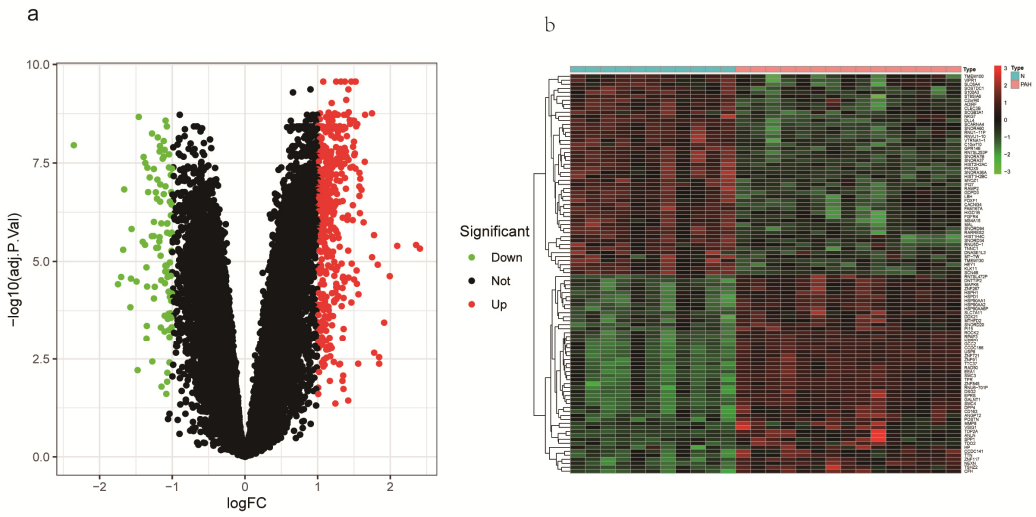

Figure 2. Differentially expressed genes identification. (a) Volcano plots of DEGs. (b) A heatmap of differentally expressed genes.

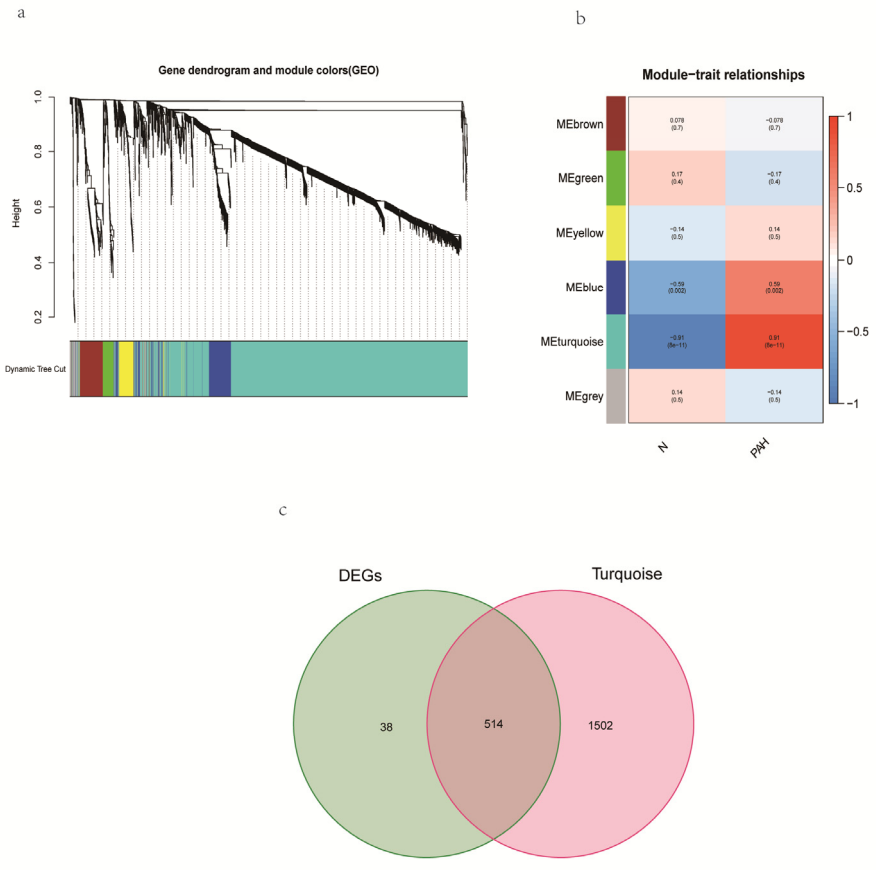

Figure 3. Weighted gene correlation network analysis. (a) Recognition module,each module was given an individual color as identifiers, including 6 different modules. (b) Correlation heat map of gene modules and phenotypes, the red is positively correlated with the phenotype, blue is negatively correlated with the phenotype. (c) Venn diagrams between DEGs and turquoise module.

3. Results

3.1. Identification of ferroptosis-associated DEGs

A total of 551 DEGs were identified (454 upregulated and 97 downregulated in the PAH group; Figure 2a, Table S1). The 50 most significant DEGs were visualized via a heatmap (Figure 2b).

3.2. WGCNA analysis

Six modules were identified using WGCNA (Figure 3b). The turquoise module included 2016 genes and was positively correlated with the PAH group (correlation = 0.91, p = 8e-6; Figure 3b). We identified 514 key DEGs in the intersection of the turquoise module and DEGs (Figure 3c).

3.3. Screening for ferroptosis-associated genes

The intersection of key DEGs and ferroptosis-associated genes consisted of eight genes, including four drivers (IDH1, DPP4, HIF1A and ACSL4), three suppressors (SLC7A11, HIF1A, and PLIN2), and three markers (EIF2S1, SLC7A11 and TXNRD1) respectively (Figure 4). The boxplots demonstrated upregulation of all these genes in the PAH group (Figure 5).

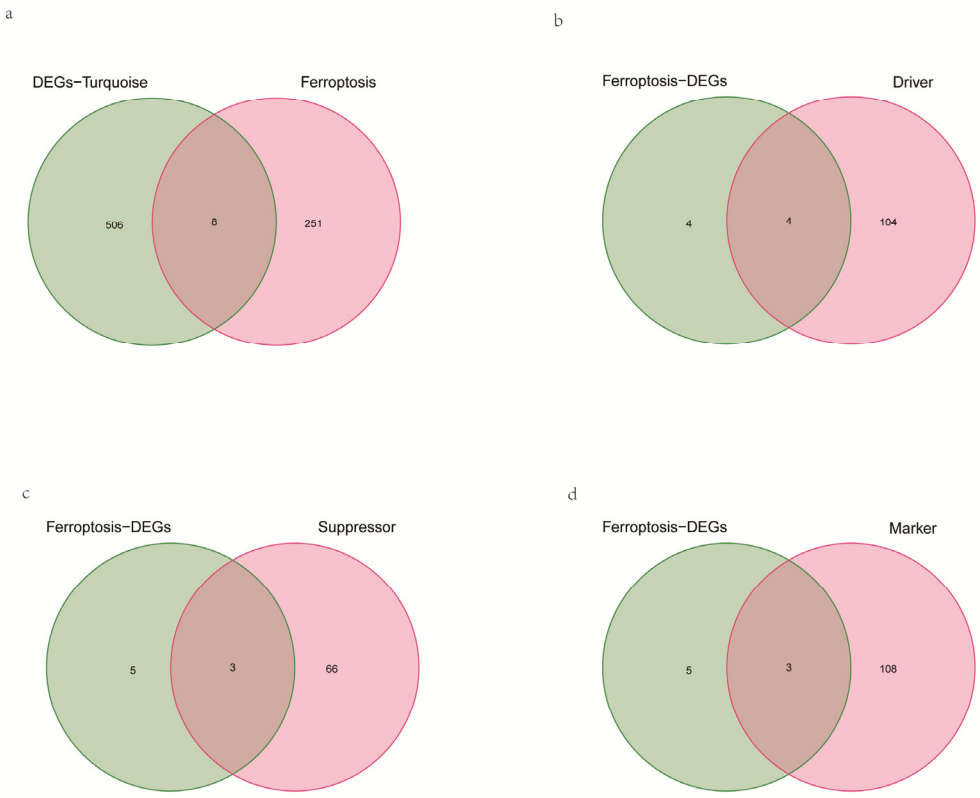

Figure 4. Venn diagrams of (a) ferroptosis-related genes (b) Driver genes of ferroptosis-related genes (c) Suppress genes of ferroptosis-related genes (d) Marker genes of ferroptosis-related genes.

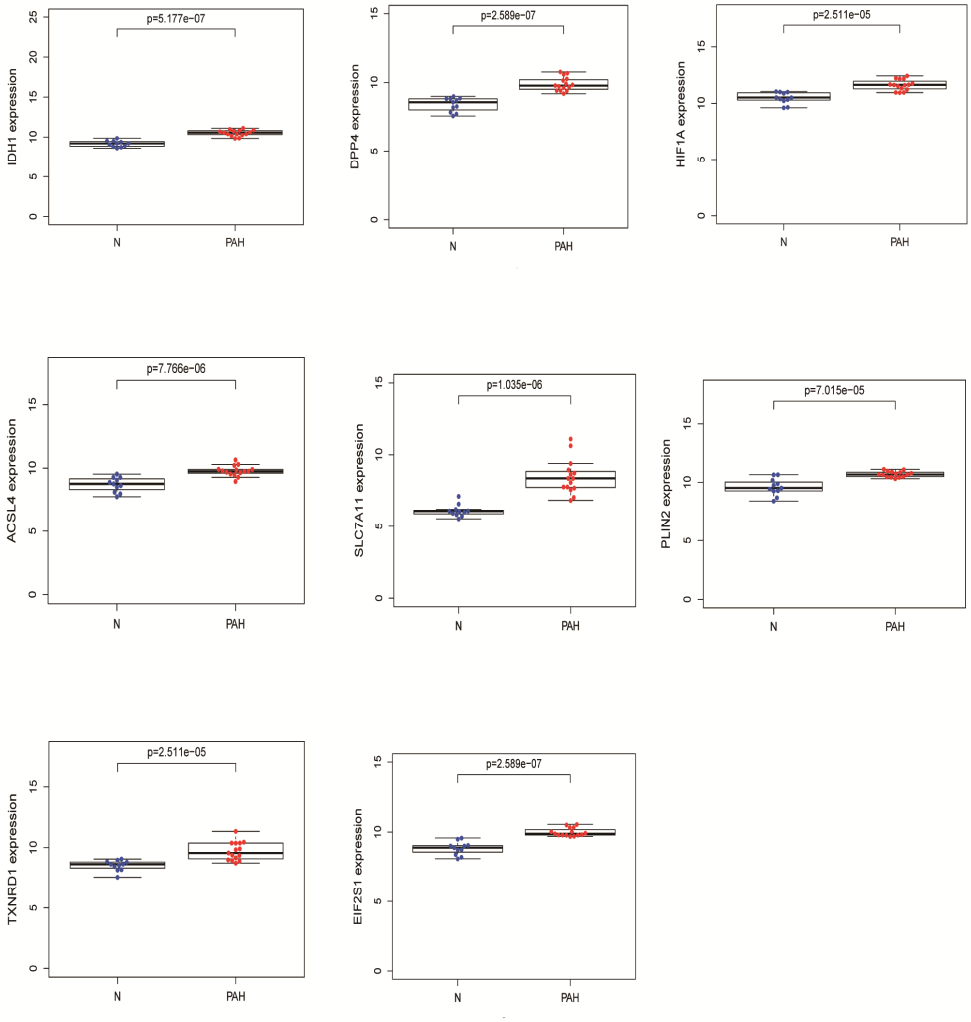

Figure 5. Ferroptosis-related genes are up-regulated in PAH group.

3.4. Correlations between the expression patterns of ferroptosis-associated genes

Driver expression levels exhibited a strong positive correlation with the expression levels of a number of other ferroptosis-associated genes: DPP4 expression correlated with that of IDH1, ACSL4 and PLIN2, whereas IDH1 expression correlated with the expression of both PLIN2 and EIF2S1. In addition, expression levels of the suppressor HIF1A and PLIN2 exhibited a strong positive correlation with that of the marker EIF2S1 (Figure 6a).

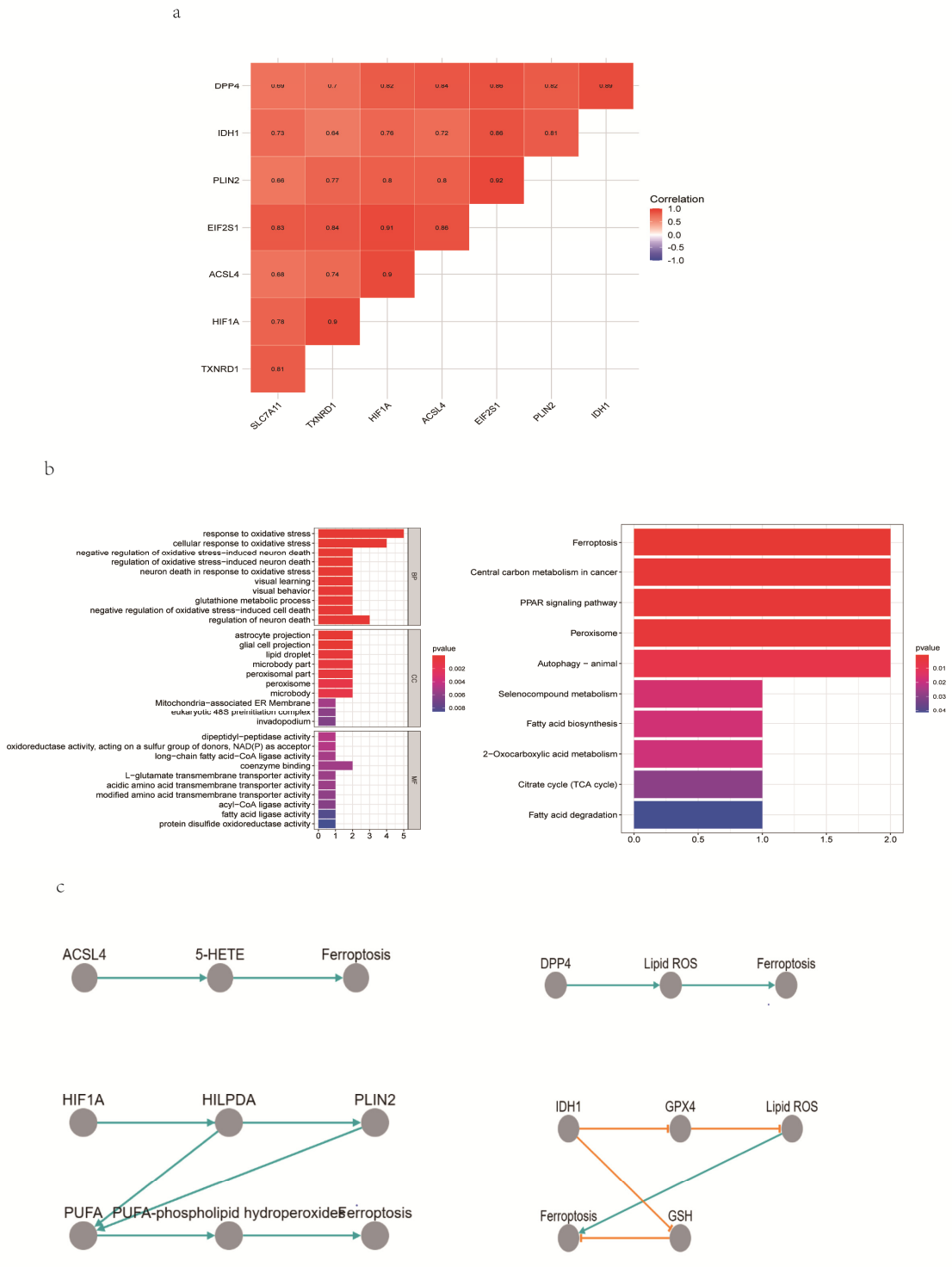

Figure 6. The potential mechanism of ferroptosis in PAH. (a) The correlation between ferroptosis-related genes, blue indicates negative correlation and red indicates positive correlation. (b) GO and KEGG enrichment analysis. (c) Pathway of ferroptosis-related genes, the arrow represents promotion and the vertical line represents inhibition.

3.5. Functional enrichment analysis

The identified ferroptosis-associated genes were significantly enriched for multiple GO biological process terms indicating: response to oxidative stress, cellular response to oxidative stress, negative regulation of oxidative stress-induced neuron death, regulation of oxidative stress-induced neuron death, neuron death in response to oxidative stress and regulation of neuron death (Figure 6b). As well as, various GO molecular function terms including, but not limited to coenzyme binding,oxidoreductase activity, acting on a sulfur group of donors, NAD(P) as an acceptor, dipeptidyl-peptidase activity and acyl-CoA ligase activity (Figure 6b). The KEGG pathways analyses suggested the involvement of ferroptosis-associated genes enriched in ferroptosis and peroxisome (Figure 6b). The pathway maps for the drivers and suppressors are shown in Figure 6c.

3.6. Gene-miRNA and gene-TF network analysis

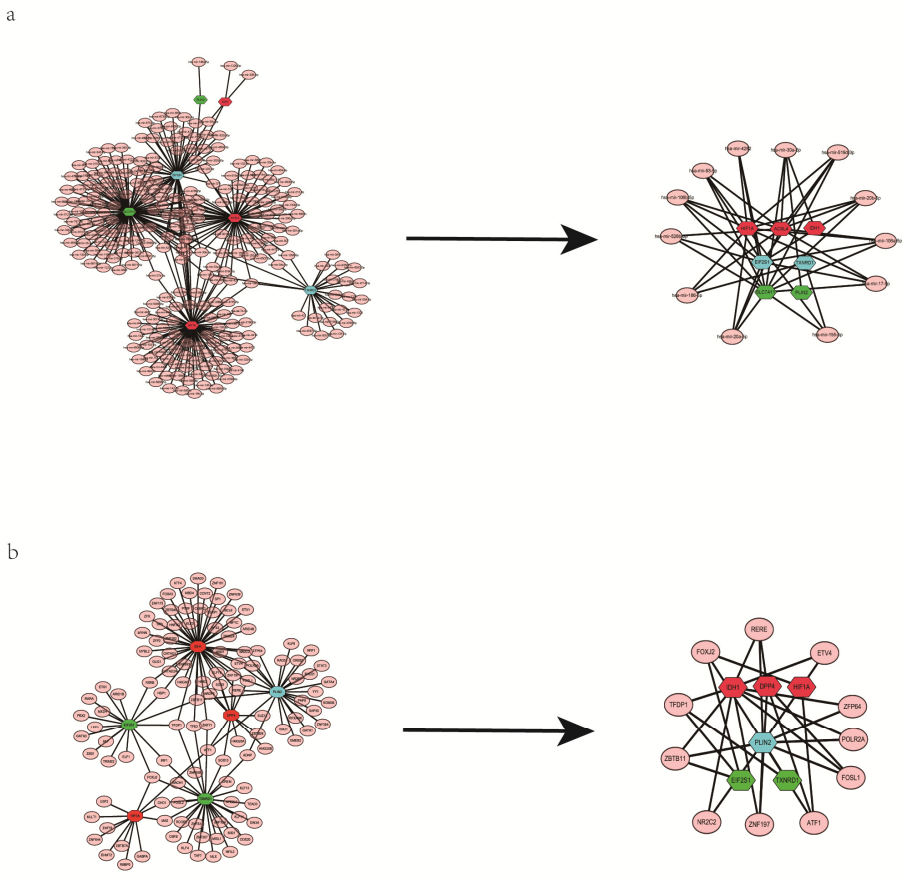

Figure 7. Gene-miRNA network and Gene-TF network. (a) Red indicates driver gene, green indicates suppress gene, blue indicates marker gene, pink indicates miRNA. (b) Red indicates driver gene, green indicates suppress gene, blue indicates marker gene, pink indicates TF.

The gene-miRNA network demonstrated that three drivers, two suppressors, and two markers were simultaneously regulated by hsa-mir-30a-5p, hsa-mir-519d-3p, hsa-mir-20b-5p, hsa-mir-106a-5p, hsa-mir-17-5p, hsa-mir-17-5p, hsa-mir-20a-5p, hsa-mir-186-5p, hsa-mir-526b-3p,

hsa-mir-106b-5p, hsa-mir-93-5p and hsa-mir-4282. Therefore, we speculated these miRNAs were involved in regulation of ferroptosis in the context of PAH (Figure 7a). The gene-TF network suggested that three drivers and multiple suppressors and markers were regulated by FOXJ2, RERE, ZFP64, POLR2A, FOSL1, ATF1, ZNF197, ZBTB11 and TFDP1 (Figure 7b).

4. Discussion

We systematically investigated the functions and regulation of eight ferroptosis-associated genes demonstrating significantly altered expression in PAH. Expression of all ferroptosis-associated genes was upregulated in PAH group, including three markers. This strongly suggests that PAH causes the occurrence of ferroptosis within lung tissues.

With regard to the potential regulatory mechanisms controlling PAH-associated ferroptosis, the upregulated expression of three suppressor genes suggests that promotion and restraint of ferroptosis coexist. Additionally, all ten ferroptosis-associated genes exhibited positively correlated expression patterns, suggesting possible co-regulation of these genes. That the expression of the driver IDH1 correlates particularly strongly with the expression of the suppressor PLIN2 further supports the coexistence of ferroptosis initiation and regulation. However, based on upregulated expression of multiple marker genes, ferroptosis was activated overall.

As regards the potential molecular mechanisms underlying PAH-associated ferroptosis, enrichment analysis results suggested the involvement of ferroptosis-associated genes in oxidative stress-induced neuron death. Therefore, we speculated that PAH-associated ferroptosis was associated with oxidative stress- induced neuron death by the ferroptosis pathway. Oxidative stress is a major predisposing factor of some lung diseases: chronic obstructive pulmonary disease (COPD), idiopathic pulmonary fibrosis (IPF), and acute respiratory distress syndrome (ARDS) [24,25]. Oxidative stress in the cell is characterized by the excessive generation of reactive oxygen species (ROS) [26]. Disturbed blood flow in PAH stimulates numerous signaling pathways leading to oxidative stress, expression of atherogenic factors, and endothelial dysfunction [27]. Cellular accumulation of oxidant-induced lipid peroxidation is the major mechanism causing iron-dependent ferroptosis [4,28]. Our pathway map (Figure 6c) suggested that ROS play a key role in the pathway of ferroptosis.

MiRNAs play important roles in diverse fundamental biological processes [29,30]. For example, miR-137 negatively regulates ferroptosis via direct targeting of the glutamine transporter SLC1A5 in melanoma cells [31]. The gene-miRNA network we constructed in the present study suggested that 12 miRNAs simultaneously regulated multiple ferroptosis-associated genes in the context of PAH. Additionally, TFs are key regulators of cellular gene expression [32], and are implicated in the pathogenesis of various diseases. For example, 164 TFs are thought to be directly involved in 277 diseases [33]. Our gene-TF network indicated that nine TFs control the expression of multiple ferroptosis-associated genes exhibiting PAH expression. These findings suggested that these TFs may be the major elements regulating the expression of ferroptosis-associated genes.

5. Conclusions

Collectively, our findings suggested that PAH initiated lung tissue ferroptosis, which may be associated with oxidative stress responses, and was likely subjected to modulatable regulation by the

identified miRNAs and TFs. Despite certain limitations [e.g., the FerrDb knowledgebase reflects mRNA levels in a relatively small dataset (n = 10)], we provided the initial evidence supporting this novel direction for the targeted therapy of PAH. Although the appropriate pharmaceutical compounds for inhibiting ferroptosis may not exist yet, inhibition of ferroptosis may improve the therapeutic outcomes of patients with PAH. In future studies, we would like to validate these findings at the protein expression level in a larger cohort, and to confirm that ferroptosis indeed occurs *in vivo*. We also intend to examine peripheral blood for an increase in the circulating levels of markers of ferroptosis (end products of lipid peroxidation; reactive aldehydes, such as malondialdehyde and 4-hydroxynonenal) in PAH patients.

Acknowledgments

We acknowledge GEO database for providing their platforms and contributors for uploading their meaningful datasets.

We would like to thank Editage (www.editage.cn) for English language editing

Conflict of interest

None of the authors declare any potential conflict of interest.

References

1. G. Mansueto, M. D. Napoli, C.P. Campobasso, M. Slevin, Pulmonary arterial hypertension (PAH) from autopsy study: T-cells, B-cells and mastocytes detection as morphological evidence of immunologically mediated pathogenesis, *Pathol. Res. Pract*., **225** (2021), 153552.
2. S. Gräf, M. Haimel, M. Bleda, C. Hadinnapola, L. Southgate, W. Li, et al., Identification of rare sequence variation underlying heritable pulmonary arterial hypertension, *Nat. Commun*., **9** (2018), 1416.
3. T. Hiraide, M. Kataoka, H. Suzuki, Y. Aimi, T. Chiba, K. Kanekura, et al., SOX17 Mutations in Japanese Patients with Pulmonary Arterial Hypertension, *Am. J. Respir. Crit. Care Med*., **198** (2018), 1231–1233.
4. S. J. Dixon, K. M. Lemberg, M. R. Lamprecht, R. Skouta, E. M. Zaitsev, C. E. Gleason, et al., Ferroptosis: an iron-dependent form of nonapoptotic cell death, *Cell*, **149** (2012), 1060–1072.
5. Y. C. Li, Y. M. Cao, J. Xiao, J. W. Shang, Q. Tan, F. Ping, et al., Inhibitor of apoptosis-stimulating protein of p53 inhibits ferroptosis and alleviates intestinal ischemia/reperfusion-induced acute lung injury, *Cell Death Differ.*, **27** (2020), 2635–2650.
6. X. Li, L. J. Duan, S. J. Yuan, X. B. Zhuang, T. K. Qiao, J. He, Ferroptosis inhibitor alleviates Radiation-induced lung fibrosis (RILF) via down-regulation of TGF-β1, *J. Inflamm. (Lond).*, **16** (2019), 11.
7. M. Mura, M. J. Cecchini, M. Joseph, J. T. Granton, Osteopontin lung gene expression is a marker of disease severity in pulmonary arterial hypertension, *Respirology*, **24** (2019), 1104–1110.
8. T. Barrett, S. E. Wilhite, P. Ledoux, C. Evangelista, I. F. Kim, M. Tomashevsky, et al., NCBI GEO: archive for functional genomics data sets--update, *Nucleic Acids Res.*, **41** (2013), D991–D995.

9. H. Jalal, P. Pechlivanoglou, E. Krijkamp, F. Alarid-Escudero, E. Enns, M. G. M. Hunink, An overview of R in health decision sciences, *Med. Decis. Making*, **37** (2017), 735–746.
10. M. E. Ritchie, B. Phipson, D. Wu, Y. F. Hu, C. W. Law, W. Shi, et al., Limma powers differential expression analyses for RNA-sequencing and microarray studies, *Nucleic Acids Res.*, **43** (2015), e47.
11. K. Ito, D. Murphy, Application of ggplot2 to Pharmacometric Graphics, *CPT Pharmacometrics Syst. Pharmacol.*, **2** (2013), 1–16.
12. R. Kolde, Pheatmap: pretty heatmaps, R package version, 1.0.8., 2015. Available from: https://CRAN.R-project.org/package= pheatmap.
13. P. Langfelder, S. Horvath, WGCNA: an R package for weighted correlation network analysis, *BMC Bioinf.*, **9** (2008), 559.
14. H. B. Chen, P.C. Boutros, VennDiagram: a package for the generation of highly-customizable Venn and Euler diagrams in R, *BMC Bioinf.*, **12** (2011), 35.
15. N. Zhou, J. K. Bao, FerrDb: a manually curated resource for regulators and markers of ferroptosis and ferroptosis-disease associations, *Database*, **2020** (2020).
16. A. Eklund, Beeswarm: the bee swarm plot, an alternative to stripchart, R package version, 0.2.3., 2016. Available from: https://cran.r-project.org/package= beeswarm.
17. H. A. Kassambara, Ggpubr: "ggplot2" based punlication ready plots, R package version, 1.0.7., 2018. Available from: https:// cran.r-project.org/install.packages ("ggpubr").
18. G. C. Yu, L. G. Wang, Y. Y. Han, Q. Y. He, clusterProfiler: an R package for comparing biological themes among gene clusters, *Omics: J. Integr. Biol.*, **16** (2012), 284–287.
19. B. Nota, Gogadget: An R package for interpretation and visualization of GO enrichment results, *Mol. Inf.*, **36** (2017), 5–6.
20. M. Kanehisa, M. Furumichi, M. Tanabe, Y. Sato, K. Morishima, KEGG: new perspectives on genomes, pathways, diseases and drugs, *Nucleic Acids Res*., **45** (2017), D353–D361.
21. S. D. Hsu, F. M. Lin, W. Y. Wu, C. Liang, W. C. Huang, W. L. Chan, et al., miRTarBase: a database curates experimentally validated microRNA-target interactions, *Nucleic Acids Res.*, **39** (2011), D163–D169.
22. J. R. Ecker, W. A. Bickmore, I. Barroso, J. K. Pritchard, Y. Gilad, E. Segal, Genomics: ENCODE explained, *Nature*, **489** (2012), 52–55.
23. J. Reimand, R. Isserlin, V. Voisin, M. Kucera, C. Tannus-Lopes, A. Rostamianfar, et al., Pathway enrichment analysis and visualization of omics data using g: Profiler, GSEA, Cytoscape and EnrichmentMap, *Nat. Protoc.*, **14** (2019), 482–517.
24. L. Hecker, Mechanisms and consequences of oxidative stress in lung disease: therapeutic implications for an aging populace, *Am. J. Physiol. Lung Cell Mol. Physiol*., **314** (2018), L642–L653.
25. P. A. Kirkham, P. J. Barnes, Oxidative stress in COPD, *Chest*, **144** (2013), 266–273.
26. E. A. Zemskov, Q. Lu, W. Ornatowski, C. N. Klinger, A. A. Desai, E. Maltepe, et al., Biomechanical forces and oxidative stress: implications for pulmonary vascular disease, *Antioxid. Redox Signaling*, **31** (2019), 819–842.
27. S. Aggarwal, C. M. Gross, S. Sharma, J. R. Fineman, S. M. Black, Reactive oxygen species in pulmonary vascular remodeling, *Compr. Physiol*., **3** (2013), 1011–1034.
28. W. S. Yang, B. R. Stockwell, Ferroptosis: death by lipid peroxidation, *Trends Cell Biol*., **26** (2016), 165–176.

29. L. B. Frankel, A. H. Lund, MicroRNA regulation of autophagy, *Carcinogenesis*, **33** (2012), 2018–2025.
30. D. P. Bartel, MicroRNAs: genomics, biogenesis, mechanism, and function, *Cell*, **116** (2004), 281–297.
31. M. Y. Luo, L. F. Wu, K. X. Zhang, H. Wang, T. Zhang, L. Gutierrez, et al., miR-137 regulates ferroptosis by targeting glutamine transporter SLC1A5 in melanoma, *Cell Death Differ*., **25** (2018), 1457–1472.
32. X. L. Lai, A. Stigliani, G. Vachon, C. Carles, C. Smaczniak, C. Zubieta, et al., Building transcription factor binding site models to understand gene regulation in plants, *Mol. Plant*., **12** (2019), 743–763.
33. J. M. Vaquerizas, S. K. Kummerfeld, S. A. Teichmann, N. M. Luscombe, A census of human transcription factors: function, expression and evolution, *Nat. Rev. Genet*., **10** (2009), 252–263.

AIMS Press